Original Article

Preparation of doxorubicin-loaded collagen-PAPBA nanoparticles and their anticancer efficacy in ovarian cancer

Haiyan Jiang[1,2#], Guiwen Liang[2#], Min Dai[1], Yansong Dong[3], Yao Wu[3], Luzhong Zhang[3], Qinghua Xi[1], Lei Qi[1,2]

[1]Department of Obstetrics and Gynecology, [2]Department of Emergency Medicine, Affiliated Hospital of Nantong University, Nantong, China; [3]School of Medicine, Nantong University, Nantong, China

Contributions: (I) Conception and design: Q Xi, L Qi; (II) Administrative support: G Liang, L Zhang; (III) Provision of study materials or patients: H Jiang; (IV) Collection and assembly of data: M Dai, Y Dong, Y Wu; (V) Data analysis and interpretation: H Jiang; (VI) Manuscript writing: All authors; (VII) Final approval of manuscript: All authors.

[#]These authors contributed equally to this work as the first authors.

Correspondence to: Qinghua Xi; Lei Qi. Department of Obstetrics and Gynecology, Affiliated Hospital of Nantong University, Nantong, China. Email: ntdxfsyyxqh@163.com; qilei723@ntu.edu.cn.

Background: The aims of this study were to prepare the collagen-poly (3-acrylamidophenylboronic acid) nanoparticles (collagen-PAPBA NPs) encapsulating doxorubicin (DOX) and research their anticancer efficacy in ovarian cancer.

Methods: Collagen-PAPBA NPs were prepared, and their morphology and stability morphology were observed by transmission electron microscopy (TEM) and dynamic light scattering system (DLS). Preparation of doxorubicin-loaded Collagen-PAPBA NPs (DOX-loaded NPs) were then prepared, and the drug-loading content, encapsulation efficiency, and *in vitro* drug-release profiles were calculated. The morphology of DOX-loaded NPs was also observed by DLS, *in vitro* cytotoxicity to A2780 cells was analyzed by 3-(4,5-dimethylthiazol-2-yl)-2,5-diphenyl tetrazolium bromide (MTT) assay, *in vitro* antitumor activity on A2780 cells was observed by immunofluorescence, and *in vivo* antitumor activity was assessed using an experimental BALB/c mice tumor model.

Results: DOX-encapsulating collagen-PAPBA NPs were successfully prepared with mediation by biomolecule. The average hydrodynamic diameter of collagen-PAPBA NPs as measured by DLS was about 79 nm, with a homogeneous distribution of size. TEM revealed that nanoparticles were well-dispersed, spherical, and a roughly uniform 75 nm in size. Collagen-PAPBA NPs were quite stable in a wide range of pH and temperature conditions and associated with the concentration of glucose. DLS revealed that the average hydrodynamic diameter of DOX-loaded NPs was about 81.3 nm, with homogeneous distribution of size. TEM revealed that drug-loaded nanoparticles were spherical, well-dispersed, and gad a roughly uniform size of 79 nm. The proportion of DOX loaded into the nanoparticles was 10%, while the encapsulating efficiency was 97%. The result of the releasing test showed that the drug-loaded nanoparticles, as carriers for DOX, had a good sustained-release effect. The cell toxicity experiment showed that the blank NPs had no cytotoxicity to A2780 cells, and that the drug-loaded NPS had good a sustained-release function. They may thus have potential toxic-reducing side effects.

Conclusions: Under the same doses, the drug-loaded NP had a superior inhibitory effect to free DOX on the growth of human ovarian cancer.

Keywords: Doxorubicin; collagen; nanoparticles; drug delivery; ovarian cancer

Submitted Jun 03, 2020. Accepted for publication Jul 13, 2020.
doi: 10.21037/atm-20-5028
View this article at: http://dx.doi.org/10.21037/atm-20-5028

Introduction

Ovarian cancer is the fifth most prevalent cancer among women, and, mainly owing to its late-stage diagnosis, is the most lethal gynecologic malignancy, often resulting in death (1). The 5-year survival rate of advanced stage ovarian cancer patients is presently about only 30% (2). The poor prognosis of patients with drug-resistant ovarian cancer and the lack of targeted therapy have raised the need for alternative treatments (3). In the last few decades, new treatment modalities with improved diagnostic methods and surgical techniques have been established, but only a marginal improvement in survival has been gained (4). Most patients will ultimately recur and succumb to their disease. Current ovarian cancer treatment involves chemotherapy which helps to improve the overall survival of these patients (5). The clinical treatment of ovarian cancer involves an array of chemotherapeutic drugs, including doxorubicin (DOX), decitabine, cisplatin, cyclophosphamide, carboplatin, paclitaxel, gemcitabine, and their combination (6,7). Unfortunately, traditional chemotherapy has inevitable drawbacks including high toxicity, poor therapeutic efficiency, and nonspecific tumor targeting (8,9). There is therefore an urgent need to identify new therapeutic agents which can improve the efficacy of existing therapeutic modalities.

Nanotechnology, as a rapidly growing field, has seen several breakthroughs in recent years, with its pharmacokinetic properties showing promise for the diagnosis and treatment of cancer (10). Nanotechnology, in the form of nanomedical products, has improved the therapeutic strategies against cancer (11) and has demonstrated enhanced efficacy and reduced toxicity (8). Because of the subcellular and submicron size of the nanoparticle-based drug delivery system, it can easily permeate deeply into tissues and fine capillaries (12). In particular, natural polysaccharides based bio-nanoparticles are widely used as delivery systems for treatments like anti-inflammatory drugs (13), antibiotics (14), proteins (15), genes (16), peptides (17), and hormones (18), all due to their remarkable superiority in biodegradability and biocompatibility (19). Among them, liposomal doxorubicin has achieved good treatment effects in ovarian cancer patients (20). These modified polysaccharides can self-assemble into nanoparticles with the hydrophobic segments forming the core and hydrophilic segments forming the shell in the aqueous solution (21). These polysaccharide-based nanodrug delivery systems have significant value in being able to stabilize therapeutic agents, improve the solubility of hydrophobic drugs, prolong circulation life-time, and reduce the side effects of the drugs (22). Due to its many advantageous properties, collagen has been utilized as a scaffold for tissue engineering applications (23). However, collagen is mechanically weak, and, in its purified state, is prone to rapid degradation (24). Fortunately, collagen can be cross-linked to mitigate these effects (25). While stability and enhanced mechanical properties can be achieved through crosslinking, it may also render collagen less biocompatible either due to the cytotoxicity of the crosslinkers or due to the changes in the overall microstructure (23,25). In our previous work, we reported a simple method to prepare a synthesis of methylprednisolone-loaded ibuprofen-modified dextran-based nanoparticles (NPs) (26). From these NPs, collagen-containing NPs were prepared by polymerizing 3-acrylamidophenylboronic acid (APBA) monomer in an aqueous solution of collagen. The present study aimed to prepare doxorubicin-encapsulating collagen-PAPBA nanoparticles and to evaluate their anticancer efficacy in ovarian cancer. In this system, through a reversible boronic acid-diol reaction, collagen interacts with boronic groups, and this has been demonstrated and monitored by 11B-Nuclear Magnetic Resonance(NMR). The NPs remain stable over a wide range of pH and temperature conditions and show a relatively narrow size distribution. The size and composition of the NPs can be easily regulated by changing the feeding ratio of collagen to PAPBA. Herein, we report the *in vivo* behaviors of the DOX-loaded collagen-PAPBA NPs and their antitumor performance on an ovarian cancer model. The results demonstrate that the DOX-loaded NPs had significantly better efficacy in impeding tumor growth than free DOX.

We present the following article in accordance with the ARRIVE reporting checklist (available at http://dx.doi.org/10.21037/atm-20-5028).

Methods

Synthesis of 3-acrylamidophenylboronic acid

First, 5.16 g sodium hydroxide was dissolved in double-distilled water into a 50 mL solution, and 5.0 g (32.2 mmol) 3-aminophenylboronic acid was dissolved into the solution. In cautious, dropwise fashion, 5.2 mL (64.4 mmol) acryloyl chloride was stirred into the coolant in 10 minutes and stirred for 30 min, allowing the reaction to reach

room temperature. The mixture was adjusted to pH 8 by hydrochloric acid. The precipitate was obtained by filtration, washed by 25 mL cold water, and then dried. The resulting solid was dissolved into a hot 50 mL ethanol water solution (Vethanol: Vwater =80:20). The filtrate was rested overnight and filtered, and the white solids were isolated and dried.

Preparation of collagen-PAPBA NPs

Briefly, 120 mg of collagen-I and 90 mg of 3-acrylamidophenylboronic acid were dissolved into 10 mL of water by heating. After this, 9.4 mg of 4,4-azobis (4-cyanovaleric acid) was added, and the pH value of the resulting solution was adjusted to ca. 6.3 with sodium hydroxide solution. The resulting mixture was stirred at 90 ℃. When the reaction mixture became blue, the reaction was allowed to continue for another 2 hours. The prepared NPs were purified by dialysis against 1 L of deionized water in a 100 kDa molecular weight cut-off (MWCO) membrane for 10 hours and collected after lyophilization.

Morphology of collagen-PAPBA NPs

The morphology of the nanospheres was observed by transmission electron microscopy (TEM, JEM-1010, Japan). A drop of the nanoparticles was dispersed on a copper mesh covered with nitrocellulose nitrate membrane and dried in air. Atomic force microscopy was used to observe the surface of the nanoparticles. A drop of dispersion liquid was dropped on a clean silicon wafer, dried with nitrogen, and then scanned in a tapping pattern using 20 μm.

Stability of collagen-PAPBA NPs

A Brookheaven BI-9000AT dynamic light scattering system (DLS, Brookheaven Instruments Corp., USA) was used in this study. Due to the sensitivity of 3-acrylamidophenylboronic acid to solution pH value, temperature and glucose, the effect of different pH values, temperatures, and concentrations of glucose on collagen-PAPBA NPs was investigated. The pH value was set to 4, 5, 6, 7.4, 8.5, and 10. The temperature was set to 25, 30, 35, 40, 45, 50, and 55 ℃. Concentrations of glucose were set to 0, 10 20, 40 60, 80, 120, 160, and 200 mg/mL, dissolved in phosphate-buffered saline (PBS). The solution of collagen-PAPBA NPs was adjusted to different pH values with sodium hydroxide solution and hydrochloric acid. The solution of nanoparticles was placed overnight at room temperature, and the diameter was measured by DLS. The solution of collagen-PAPBA NPs was kept at different temperatures for more than half an hour, and the diameter was measured by DLS. At room temperature, the solution of collagen-PAPBA NPs was placed overnight in different concentrations of glucose solution, and the diameter of nanoparticles was measured by DLS.

Preparation of DOX-loaded collagen-PAPBA NPs

A DOX aqueous solution (3 mg/mL, 1 mL) was added to a stirred suspension of collagen-PAPBA NPs in water (5 mg/mL, 5 mL) in which the pH was adjusted to 8.4 with sodium hydroxide solution beforehand. The resulting mixture was stirred for 12 hours. Thereafter, the mixture was centrifuged at 10,000 r/min for 30 min to remove the free DOX. The precipitation was redispersed into a predetermined volume of glucose injection, yielding a suspension of DOX-loaded collagen-PAPBA NPs.

Drug-loading content and encapsulation efficiency

The prepared acid of DOX-loaded NPs was centrifuged at high speed (30,000 rmp/min) for 30 min, and the supernatant solution was used to test the concentration of DOX which was not encapsulated in the nanoparticles. The solid was dried out, and the general quantity was determined. The amount of DOX was detected by fluorescence chromatography. The drug-loading content and encapsulation efficiency were respectively calculated by the following formulas:

$$\text{Drug - loading content } \% = \frac{\text{Weight of the drug in the nanoparticles}}{\text{Weight of the nanoparticles}} \times 100\% \quad [1]$$

$$\text{Encapsulation efficiency } \% = \frac{\text{Weight of drug in the nanoparticles}}{\text{Weight of the feeding drug}} \times 100\% \quad [2]$$

Morphology of DOX-loaded NPs

A Brookheaven BI-9000AT dynamic light scattering system (DLS, Brookheaven Instruments Corp., USA) and a LSM-710 laser scanning confocal microscope (ZEISS, Germany) were used to measure the size of DOX-loaded NPs. The incident angle was 90 degrees, and the incident wavelength of the laser was 633 nm. Each sample was measured 3 times, 60 times per scan. The concentrations of the samples were measured at 0.05%. The test temperature was room temperature, and the average diameter of the particle was presented as mean ± standard deviation (SD). The

morphology of the nanospheres was also observed by TEM. A drop of the nanoparticles was dispersed on the copper mesh covered with nitrocellulose nitrate membrane and dried in air. Atomic force microscopy was used to observe the surface of the nanoparticles. A drop of dispersion liquid was dropped on a clean silicon wafer, dried with nitrogen, and then scanned in a tapping pattern using 20 μm.

In vitro drug-release profiles of the DOX-loaded NPs

A 12 kDa MWCO membrane was used to dialyze the aqueous suspension of the DOX-loaded NPs with 10 mL of PBS at 37 ℃. At a specific time point (0, 3, 6, 9, 12, 18, 24, 48, 96, 120, 144, and 168 hours), a sample (1 mL) of aliquot was taken out from the bulk of PBS solution, and then the same volume (1 mL) of medium was added to the suspension. A fluorescence spectroscope with a pre-established calibration curve was used to measure the released concentrations of DOX in the sample medium. At each time point, the accumulative release percentage was calculated. The measurements were repeated three times, and the average of three measurements is presented as the result.

In vitro cytotoxicity

A 3-(4, 5-dimethylthiazol-2-yl)-2, 5-diphenyltetrazolium bromide (MTT) assay was used to test the cytotoxicity of samples. A2780 cells were grown in Dulbecco's Modified Eagle's Medium (DMEM) containing 4 mM glutamine, 100 μg/mL streptomycin, and 100 U/mL penicillin with 10% fetal bovine serum (FBS) in a 5% CO_2 atmosphere at 37 ℃. Then, the cells, at a density of 5,000 cells per well, were seeded into a 96-well plate and incubated with 100 μL of culture medium containing different doses of samples at 37 ℃ for 2 days. After being incubated, the medium in each well was removed, and PBS was used to wash the cell three times. Next, MTT solution (5 mg/mL, 10 μL) was added to each well and cultivated for 4 hours. The supernatant liquid was discarded, and 100 μL of dimethyl sulfoxide (DMSO) was subsequently added. A microplate reader (Safire, Tecan, Swiss) was used to observe the optical density (OD) of plates at 570 nm. Without further modifications after various treatments, the results were expressed as the percentage of cells relative to the control cells.

In vitro anti-tumor activity

In vitro anti-tumor activity of DOX-loaded NPs on A2780 cells was observed by immunofluorescence. The experimental steps were as follows: A2780 cells were cultured in DMEM culture containing 10% FBS. After 24 hours, a new culture medium was replaced to remove dead cells. Then, the cells, at a density of 1×10^6 cells per well, were seeded into a 6-welled plate, and incubated with 100 μL of culture medium containing different doses of samples at 37 ℃ for 2 days. The medium in each well were removed and free DOX (8 μg/mL) and the same DOX doses of DOX-loaded NPs were added and co-cultured for 2 and 4 hours. After being incubated, the medium in each well was removed, and PBS was used to wash the cell three times for 5 min. Next, the cells were fixed in 1 mL 4% paraformaldehyde for 10 min and confined by 5% bovine serum albumin (BSA) for 1 hour. Then, 0.5 mL phalloidin (12 U/mL) was added and incubated for 20 min in a dark space. PBS was used to wash the cells three times for 5 min. 4',6-diamidino-2-phenylindole was added for 3 min in a dark space, and then the co-cultured A2780 cells were mounted and examined under fluorescent microscopy (200 times magnification).

In vivo anti-tumor activity

All animal experiments were performed in accordance with the guidelines for animal experiments and approved by the Animal Care Committee of Nantong University. To establish the experimental tumor model, A2780 cells (4×10^6–6×10^6 cells per mouse) were inoculated subcutaneously into the armpit of male BALB/c mice (6–8 weeks old, provided by Central Animal Laboratory of Nantong University). The tumor growth was monitored. The DOX-loaded NPs were then injected via the tail vein at a same dose of 5 mg of free DOX per kilogram of body weight in 0.2 mL of glucose injection. The blank NPs were injected via the tail vein at a same dose of NPs of DOX-loaded NPs in 0.2 mL of glucose injection. A total of 32 mice were used in this study. To observe the tumor growth in different groups, the tumor volume was measured with a caliper. The length of tumor was recorded as a and the width as b perpendicular to a; the tumor volume was calculated as follows: $1/(2\times a\times b^2)$; the growth curve was recorded. Meanwhile, the relative tumor volume (RTV) was calculated as V_t/V_0; V_0 is the volume at the time of drug injection, and V_t is the volume at each time the tumor was calculated.

Statistical analysis

GraphPad Prism 6 statistical software was used for the

statistical analysis. Morphometric data were reported as mean ± SD. Counting data comparisons between groups were subjected to the χ^2 test. For all statistical analyses, P values <0.05 were considered to be statistically significant.

Results

Synthesis of collagen-PAPBA

Poly (3-acrylamidophenylboronic acid) (PAPBA) has an acid-base balance in aqueous solution. When it is free, it forms a triangle, while, and, when it is ionized, it forms a tetrahedron. Ionized PAPBA can produce boric acid esters with collagen. To research the interaction of collagen and PAPBA, nuclear magnetic resonance (NMR) was used to investigated the mixture with collagen and PAPBA. Interestingly, the results (*Figure 1*) showed that when pH was low (*Figure 1*, marked as 1), only one peak was detected, representing the non-ionized PAPBA and showing that there was no formation of boric acid esters. With the increase of pH (*Figure 1*, marked as 2), II peak emerged showing the formation of boric acid esters. With the increase of pH value, the peak value became higher, illustrating the increased formation of borate. When pH reached 8.4 (*Figure 1*, marked as 3), there was only the borate peak, and when the pH was higher (*Figure 1*, marked as 4), the III peak occurred, which was the ionized APBA.

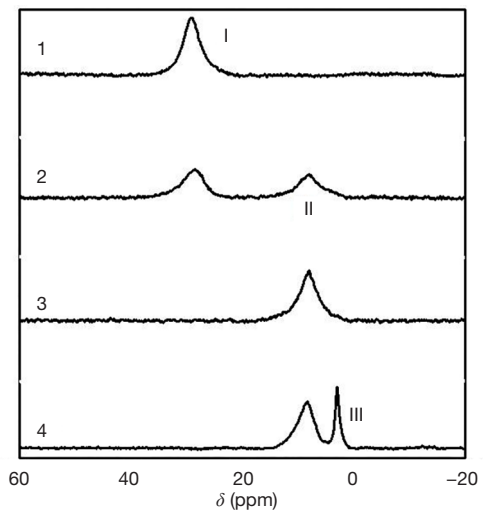

Figure 1 ^{11}B NMR spectra of collagen/APBA (the molar ratio of glucopyranoside unit to APBA is 30:1) at pH 5.6 [1], 7.4 [2], 8.4 [3], and 11.0 [4].

Morphology of collagen-PAPBA NPs

The morphology of the formed nanoparticles was examined by DLS and TEM (*Figure 2A,B*). All the collagen-PAPBA NPs exhibited an obvious spherical shape with a narrowly distributed diameter about 75 nm, which was very close to the mean diameter (79 nm) determined by the DLS.

The characterization of collagen-PAPBA NPs

Due to the sensitivity of APBA to pH, temperature, and glucose, diameters at different pH values, temperatures, and concentrations of glucose, along with zeta potential at different pH values, were tested to investigate the stability

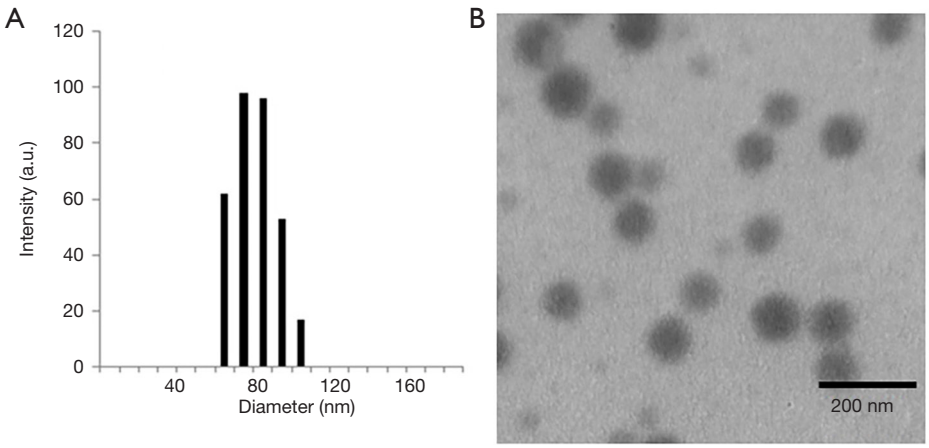

Figure 2 Images of collagen-PAPBA NPs. (A) Hydrodynamic diameter distribution of collagen-PAPBA nanoparticles; (B) typical TEM image of collagen-PAPBA NPs (the feeding molar ratio of glucopyranoside units to APBA is 2:1).

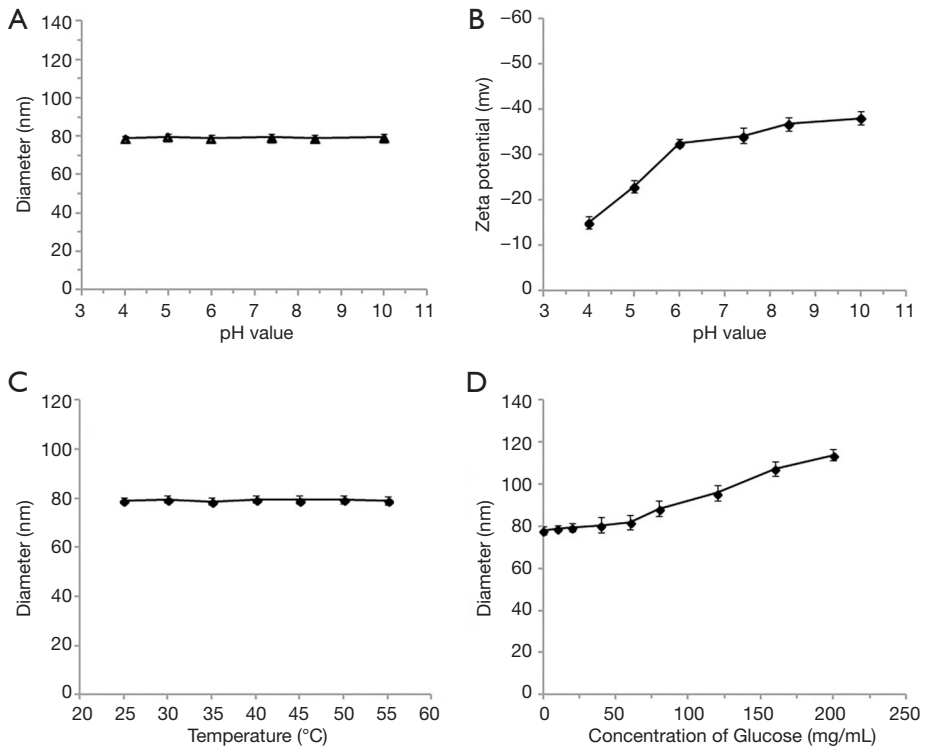

Figure 3 The characterization of collagen-PAPBA NPs. (A) The average diameter of NPs at different pH values; (B) the zeta potential of collagen-PAPBA nanoparticles at different pH values; (C) the diameter of collagen-PAPBA NPs at different temperatures; (D) the diameter of collagen-PAPBA NPs at different glucose concentrations.

of the collagen-PAPBA NPs.

Figure 3A shows the average diameter of nanospheres at different pH values. The diameter of nanospheres was unchanged between pH 4.0 to 10.0. Thus, collagen-PAPBA nanoparticles were not sensitive to the change of pH. The zeta potential of collagen-PAPBA NPs at different pH value is shown in *Figure 3B*. The zeta potential of nanospheres increased with the increase of PH. The increase of zeta potential indicated the increase of the negative charge on the surface of the nanoparticles, and the particle size became larger due to the charges repelling each other. When the pH value rose to more than 11 or decreased to less than 3, the nanoparticles could not be detected by DLS. The diameter of collagen-PAPBA nanoparticles at different temperatures is shown in *Figure 3C*. The diameter of the nanoparticles was unchanged between 24 and 35 ℃, but decreased at over 50 ℃. The diameter of collagen-PAPBA NPs at different glucose concentrations is shown in *Figure 3D*. There was no obvious change in the diameter of nanoparticles in a low concentration of glucose, but in a high concentration glucose, the diameter of nanoparticles increased rapidly as the PAPBA reacted with glucose and produced boric acid esters.

Synthesis of DOX-loaded collagen-PAPBA NPs

The morphology of collagen-PAPBA NPs was evaluated by DLS and TEM. As shown in *Figure 4A*, the diameter distribution of DOX-loaded nanoparticles was analyzed by DLS. The average size was 81.3 nm with a narrow size distribution. *Figure 4B* shows that the diameter of the nanoparticles was about 79 nm, while TEM examination shows that nanoparticles were spherical and well dispersed. The particle diameter measured by TEM was less than the hydrodynamic diameter due to the slight shrinkage of the particle size in the dry state.

In vitro release test of collagen-PAPBA NPs loaded with DOX

The release curves of collagen-PAPBA nanoparticles loaded with DOX in different pH solutions (0.01 M PBS; pH 4, 5,

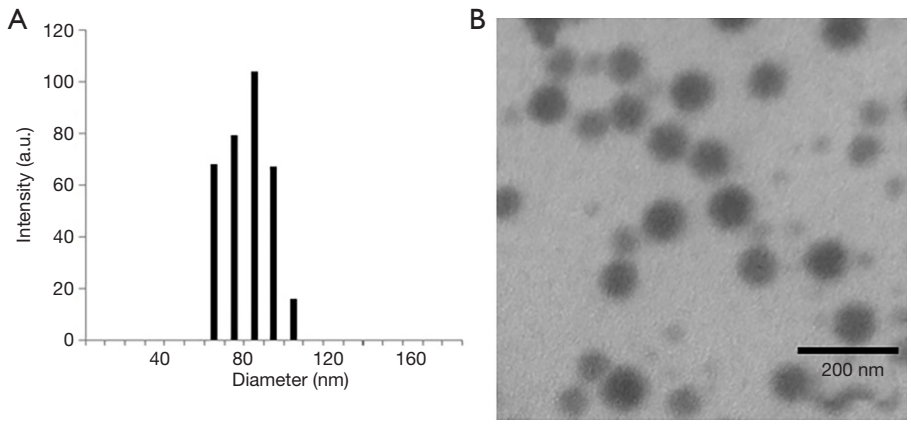

Figure 4 Morphology observation of DOX-loaded collagen-PAPBA NPs. (A) Investigation of diameter distribution of DOX-loaded collagen-PAPBA NPs loaded by DLS; (B) investigation of morphology of collagen-PAPBA NPs by TEM.

6, and 7.4, respectively) were evaluated. In acid solutions, DOX was a water soluble ion, but in alkaline solutions, DOX was a hydrophobic neutral non-ion. Therefore, we speculate that the release of DOX-loaded nanoparticles may also be sensitive to pH *in vitro*. The release curves of DOX-loaded nanoparticles in different pH solutions are shown in *Figure 5*. DOX was not released rapidly within the range of the tested pH. In a solution of pH 7.4, only about 6% of the adriamycin was released from the nanoparticles. In a solution of pH 6, the release amount increased to 19%. As the pH decreased to 5, about 33% was released from the nanoparticles. When the pH was reduced to 4, the release rate significantly increased to 76%. Therefore, we concluded that the release rate of DOX increased in acidic solution. As pH value of tumor tissue is 4 to 5, this phenomenon indicates that the drug was selective to tumor tissue. The release test showed that DOX-loaded collagen-PAPBA NPs served as a DOX antitumor drug carrier, which had sustained release effect and selective release characteristics in tumor tissue.

Drug loading and encapsulation efficiency of DOX-loaded collagen-PAPBA NPs

We measured the drug loading and encapsulation efficiency of DOX-loaded NPs. The amount of DOX encapsulation increased with the increase of pH. The pKa of DOX was 8.4, in this condition, the drug loading was 10%, and the encapsulation efficiency was 97%. This was a satisfactory result, so in the next *in vivo* and *in vitro* experiments, we use DOX-loaded collagen-PAPBA NPs prepared under this condition.

Cytotoxicity test of DOX-loaded collagen-PAPBA NPs

We then studied the cytotoxicity of blank collagen-PAPBA nanoparticles on A2780 cells *in vitro*. *Figure 6* shows the cell viability was almost 100% when the concentration of the blank nanoparticles was less than 200 g/mL. This result indicates that blank collagen-PAPBA nanoparticles (blank NPs) had no cytotoxicity to A2780 cells.

We investigated the anti-tumor effect of DOX-loaded collagen-PAPBA NPs and free DOX (0.5, 1, 2, 4, 8 μg/mL) on A2780 ovarian cancer cells *in vitro*. A2780 cells were cultured in the matrix with drug-loaded nanoparticles and free DOX for 48 hours. As shown in *Figure 7*, the cell survival rate of drug-loaded NPs (DOX NP group) was significantly lower than that of blank NPs (blank NP group) ($P<0.05$). Meanwhile, the cell survival rate of the free DOX group was lower than the cell survival rate of the DOX NP group ($P<0.05$). Thus, the cytotoxicity of DOX-loaded NPs was lower than that of the free DOX. However, when the concentration of drug-loaded NP's was higher (8 μg/mL), the cytotoxicity of the drug-loaded NP group was close to that of free DOX ($P=0.56$).

Effect of DOX-loaded collagen-PAPBA NPs on ovarian cancer in vitro

Figure 8 is a laser confocal photograph of A2780 cells co-cultured with free DOX (10 μg/mL) and DOX-loaded NPs (10 μg/mL) *in vitro* for 2 and 4 hours. Drug-loaded NPs

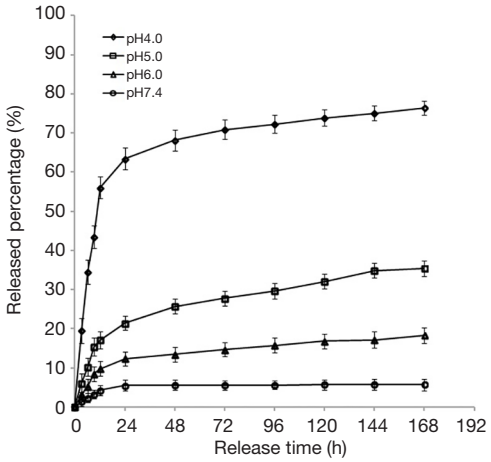

Figure 5 *In vitro* release percentage of DOX-loaded collagen-PAPBA NPs at different pH values. h, hour.

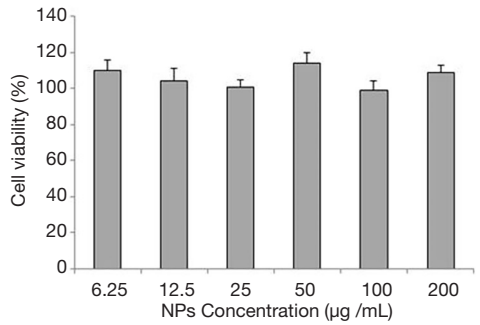

Figure 6 Cytotoxicity of different concentrations of collagen-PAPBA NPs on A2780 cells *in vitro*.

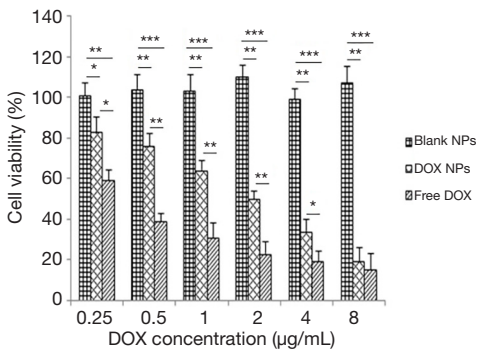

Figure 7 Cytotoxicity test of NPS loaded with different concentrations of DOX on ovarian cancer A2780 cells *in vitro*. Blank NPs, blank NPs group; DOX NPs, DOX-loaded NPs group; Free DOX, free DOX group. ***, P<0.001; **, P<0.01; *, P<0.05.

were mainly distributed in the nucleus and had an anti-tumor effect by inhibiting the synthesis of DNA and RNA. After 2 hours of co-culture, the tumor cells in the free DOX group were destroyed and the nuclei were broken, whereas the tumor cells in the DOX-loaded NP group were relatively integrated, with only a small number of nuclei ruptured (the cytoplasm was partly blue). Similar differences were found after 4 hours of co-culture. We drew the conclusion that the DOX-loaded NPs had better release efficiency compared with free DOX.

Antitumor effect of DOX-loaded collagen-PAPBA NPs in vivo

After preventive administration, the volume of tumor in normal saline group and the blank NP group increased rapidly (*Figure 9*). The growth rate of the free DOX group was lower than that of the normal saline group and the blank NP group (P<0.05), which had a certain inhibitory effect on the growth of the tumor. The growth rate of the tumor was the slowest in DOX NP group, which was significantly lower than that of the free DOX group (P<0.01). Thus, drug-loaded NPs had a good inhibitory effect on the growth of ovarian cancer subcutaneous xenograft tumor at the same dose.

Discussion

Ovarian cancer is one of the most common gynecological malignancies in the world and has one of the highest mortality rates. Due to absence of overt symptoms in the early stage and the lack of effective ways for early diagnosis, only 30% of patients are diagnosed early. The current treatment includes surgery, chemotherapy, and radiotherapy. With the continuous emergence of polymer materials and the rapid development of pharmaceuticals, nanoparticles, especially high biocompatibility, biodegradable polymer nanomaterials, have been widely used in the field of medicine. The nano-based drug-loaded system has many advantages, including a slow-releasing effect, accurate targeting, and an anti-tumor efficacy that does not injure normal cells. In this study, we successfully prepared collagen-poly (3-acrylamidophenylboronic acid) NPs using a chemical reaction of boric acid and the diol by polymerization in an aqueous solution. DOX was loaded into the nanoparticles by electrostatic interaction. The

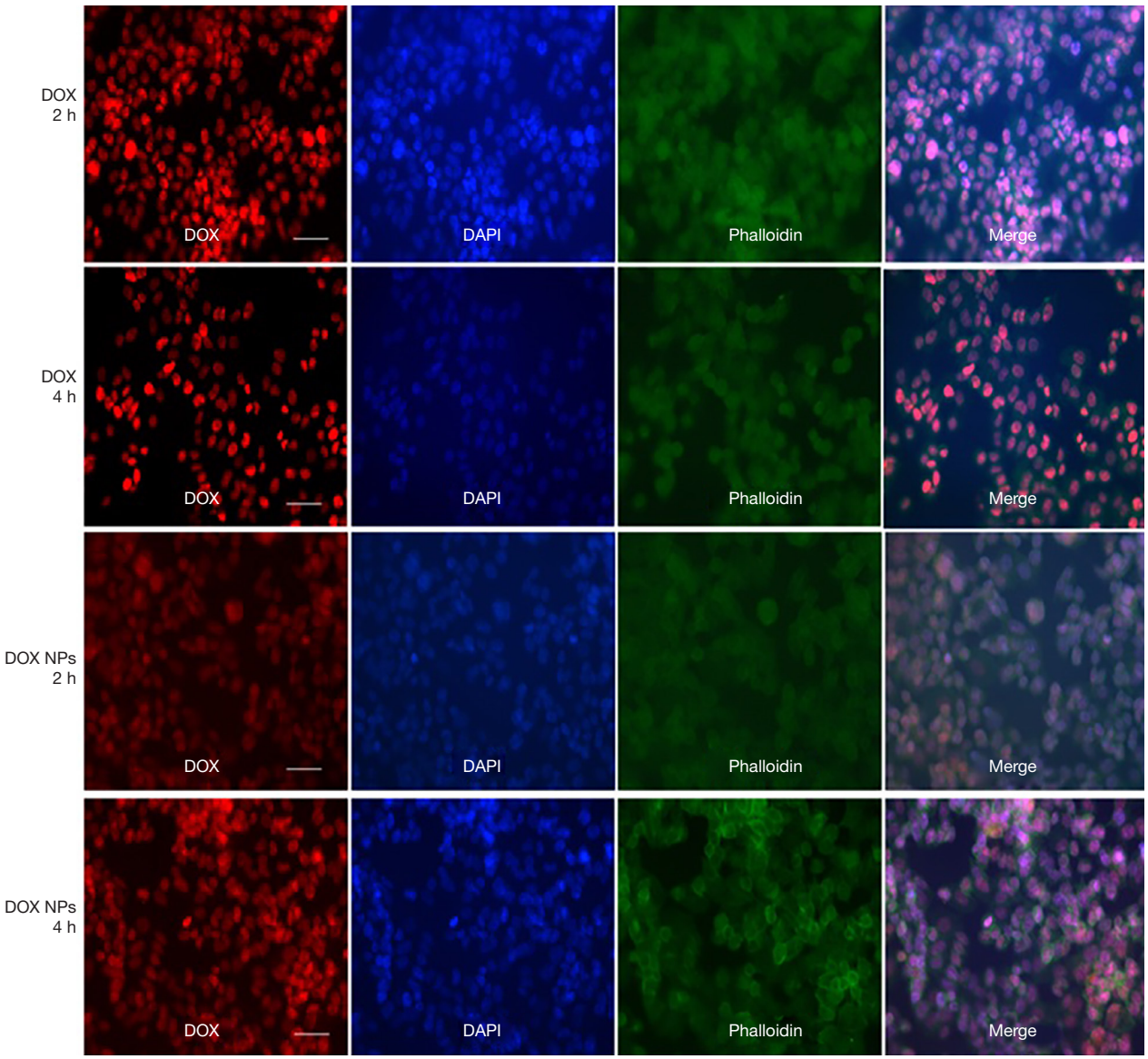

Figure 8 Immunofluorescence of A2780 cells co-cultured with free DOX and DOX-loaded nanoparticles *in vitro*. The scale is 50 μm. DOX, free DOX group; DOX NPs, DOX-loaded NPs group; h, hour.

particle size distribution and morphology of the prepared doxorubicin-loaded collagen-PAPBA nanoparticles were observed by DLS and TEM. The drug-loading and encapsulation efficiency of drug-loaded nano-microspheres were determined. A release test *in vitro*, a cytotoxicity test on ovarian cancer A2780 cells, and an antitumor effect assessment on a subcutaneous xenograft model of ovarian cancer, were conducted.

The study shows the unique anti-cancer effect of drug-loaded NPs in the animal model of ovarian cancer, which may represent a breakthrough in the treatment of ovarian cancer. However, the application of this nano-drug delivery system in ovarian cancer is still in the *in vitro* and animal experimental stage. The nano-drug delivery system has yet to be applied clinically in the field of ovarian cancer. Therefore, human experiments and in-depth studies are needed.

Despite the improvement in research of the DOX-loaded nano-based drug delivery system, several issues need to be studied before it can be clinically applied in ovarian

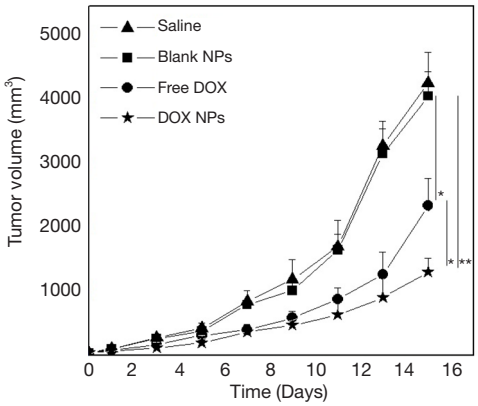

Figure 9 Antitumor effect of DOX-loaded collagen-PAPBA NPs *in vivo*. Saline, saline group; Blank NPs, blank NPs group; Free DOX, free DOX group; DOX NPs, DOX-loaded NPs group. **, P<0.01; *, P<0.05.

cancer. First, different properties and stable nano-carriers should be used to prepare the nano-based drug delivery system according to different biocompatible materials to screen the best drug carrier for ovarian cancer. Second, during the experiment, we found that the nanoparticle drug delivery system has pH sensitivity *in vitro* release, which is beneficial to the selective release of the nanoscale drug-loading system in the tumor site *in vivo*. In this study, we used a subcutaneously transplanted mice model. Because of the more representative character of the *in situ* xenograft model, we will use an orthotopic ovarian cancer model to obtain more accurate data in the future. In this study, the drug was injected in the caudal vein. In order to obtain a better anti-tumor effect, experiments with other methods of drug administration should be carried out, including those of oral administration, local administration, and tumor *in situ* administration.

The nano-based drug delivery system, as a new drug carrier, should be made more precise through the continuous development of technology to achieve a fixed point, regular, and quantitative release of drugs. Although the commercialization of the drug carrier has not yet been achieved, we firmly believe that with the development of science and technology, the nano-based drug delivery system will become an asset in the fight against disease.

Conclusions

The present study evaluated a novel DOX delivery method based on nanoparticles, prepared by the preparation of the collagen-PAPBA nanoparticles. Our research has shown that DOX-loaded collagen-PAPBA NPs have a better anticancer effect on ovarian carcinoma. We believe these DOX-loaded NP's have considerable potential in the clinical treatment of ovarian carcinoma.

Acknowledgments

Funding: This study was supported by the 2015 Maternal and Child Health Scientific Project of Jiangsu Province (F201514), the National Natural Science Foundation of China Youth Foud (81801893), and the Nantong Clinical Medicine Research Center (HS2019005).

Footnote

Reporting Checklist: The authors have completed the ARRIVE reporting checklist. Available at http://dx.doi.org/10.21037/atm-20-5028

Data Sharing Statement: Available at http://dx.doi.org/10.21037/atm-20-5028

Conflicts of Interest: All authors have completed the ICMJE uniform disclosure form (available at http://dx.doi.org/10.21037/atm-20-5028). The authors have no conflicts of interest to declare.

Ethical Statement: The authors are accountable for all aspects of the work in ensuring that questions related to the accuracy or integrity of any part of the work are appropriately investigated and resolved. This study received approval from the Ethics Committee of Affiliated Hospital of Nantong University (2019-L060). All animal experiments were performed in accordance with the guidelines for animal experiments and approved by the Animal Care Committee of Nantong University.

References

1. Jiang H, Qi L, Wang F, et al. Decreased semaphorin 3A expression is associated with a poor prognosis in patients with epithelial ovarian carcinoma. Int J Mol Med 2015;35:1374-80.
2. Jiang H, Xi Q, Wang F, et al. Increased expression of neuropilin 1 is associated with epithelial ovarian carcinoma. Mol Med Rep 2015;12:2114-20.
3. Jaragh-Alhadad L. In-vitro evaluation of HSP27 inhibitors function through HER2 pathway for ovarian cancer therapy. Transl Cancer Res 2018;7:1510-7.
4. Niu X, Rajanbabu A, Delisle M, et al. Brain metastases in women with epithelial ovarian cancer: multimodal treatment including surgery or gamma-knife radiation is associated with prolonged survival. J Obstet Gynaecol Can 2013;35:816-22.
5. Gorodnova TV, Sokolenko AP, Kuligina E, et al. Principles of clinical management of ovarian cancer. Chin Clin Oncol 2018;7:56.
6. Li SS, Ma J, Wong AST. Chemoresistance in ovarian cancer: exploiting cancer stem cell metabolism. J Gynecol Oncol 2018;29:e32.
7. Said N. Screening of three-dimensional spheroids of ovarian cancer: identification of novel therapeutics targeting stemness and chemoresistance. Ann Transl Med 2018;6:S26.
8. Yao S, Li L, Su X, et al. Development and evaluation of novel tumor-targeting paclitaxel-loaded nano-carriers for ovarian cancer treatment: in vitro and in vivo. J Exp Clin Cancer Res 2018;37:29.
9. Aina OH, Liu R, Sutcliffe JL, et al. From combinatorial chemistry to cancer-targeting peptides. Mol Pharm 2007;4:631-51.
10. Modi DA, Sunoqrot S, Bugno J, et al. Targeting of follicle stimulating hormone peptide-conjugated dendrimers to ovarian cancer cells. Nanoscale 2014;6:2812-20.
11. Opoku-Damoah Y, Assanhou A, Sooro M, et al. Functional Diagnostic and Therapeutic Nanoconstructs for Efficient Probing of Circulating Tumor Cells. ACS Appl Mater Interfaces 2018;10:14231-47.
12. Pereira de Sousa I, Moser T, Steiner C, et al. Insulin loaded mucus permeating nanoparticles: Addressing the surface characteristics as feature to improve mucus permeation. Int J Pharm 2016;500:236-44.
13. Rajitha P, Gopinath D, Biswas R, et al. Chitosan nanoparticles in drug therapy of infectious and inflammatory diseases. Expert Opin Drug Deliv 2016;13:1177-94.
14. Maleki Dizaj S, Mennati A, Jafari S, et al., Antimicrobial activity of carbon-based nanoparticles. Adv Pharm Bull 2015;5:19-23.
15. Rother M, Nussbaumer M, Renggli K, et al. Protein cages and synthetic polymers: a fruitful symbiosis for drug delivery applications, bionanotechnology and materials science. Chem Soc Rev 2016;45:6213-49.
16. Tyagi N, Arora S, Deshmukh S, et al. Exploiting Nanotechnology for the Development of MicroRNA-Based Cancer Therapeutics. J Biomed Nanotechnol 2016;12:28-42.
17. Bouttefeux O, Beloqui A, Preat V. Delivery of Peptides Via the Oral Route: Diabetes Treatment by Peptide-Loaded Nanoparticles. Curr Pharm Des 2016;22:1161-76.
18. El-Hammadi MM, Arias JL. Nano-sized platforms for vaginal drug delivery. Curr Pharm Des 2015;21:1633-44.
19. Jana S, Sen K, Gandhi A. Alginate Based Nanocarriers for Drug Delivery Applications. Curr Pharm Des 2016;22:3399-410.
20. Bun S, Yunokawa M, Tamaki Y, et al. Symptom management: the utility of regional cooling for hand-foot syndrome induced by pegylated liposomal doxorubicin in ovarian cancer. Support Care Cancer 2018;26:2161-6.
21. Rouzes C, Gref R, Leonard M, et al. Surface modification of poly(lactic acid) nanospheres using hydrophobically modified dextrans as stabilizers in an o/w emulsion/evaporation technique. J Biomed Mater Res 2000;50:557-65.
22. Zhang G, Zeng X, Li P. Nanomaterials in cancer-therapy drug delivery system. J Biomed Nanotechnol 2013;9:741-50.
23. Arkan E, Azandaryani AH, Moradipour P, et al. Biomacromolecular Based Fibers in Nanomedicine: A Combination of Drug Delivery and Tissue Engineering. Curr Pharm Biotechnol 2017;18:909-924.
24. Grant SA, Spradling CS, Grant DN, et al. Assessment of the biocompatibility and stability of a gold nanoparticle collagen bioscaffold. J Biomed Mater Res A 2014;102:332-9.
25. Zhou X, Wang J, Fang W, et al. Genipin cross-linked type II collagen/chondroitin sulfate composite hydrogel-like cell delivery system induces differentiation of adipose-derived stem cells and regenerates degenerated nucleus pulposus. Acta Biomater 2018;71:496-509.

26. Qi L, Jiang H, Cui X, et al. Synthesis of methylprednisolone loaded ibuprofen modified dextran based nanoparticles and their application for drug delivery in acute spinal cord injury. Oncotarget 2017;8:99666-80.

(English Language Editor: J. Gray)

Cite this article as: Jiang H, Liang G, Dai M, Dong Y, Wu Y, Zhang L, Xi Q, Qi L. Preparation of doxorubicin-loaded collagen-PAPBA nanoparticles and their anticancer efficacy in ovarian cancer. Ann Transl Med 2020;8(14):880. doi: 10.21037/atm-20-5028

